100 GW linear transformer driver cavity:
Design, simulations, and performance

J. D. Douglass,[*] B. T. Hutsel, J. J. Leckbee, T. D. Mulville, B. S. Stoltzfus, M. L. Wisher,
M. E. Savage, W. A. Stygar, E. W. Breden, J. D. Calhoun, M. E. Cuneo, D. J. De Smet,
R. J. Focia, R. J. Hohlfelder, D. M. Jaramillo, O. M. Johns, M. C. Jones, A. C. Lombrozo,
D. J. Lucero, J. K. Moore, J. L. Porter, S. D. Radovich, S. A. Romero, M. E. Sceiford,
M. A. Sullivan, C. A. Walker, J. R. Woodworth, and N. T. Yazzie

Sandia National Laboratories, Albuquerque, New Mexico 87185, USA

M. D. Abdalla and M. C. Skipper

ASR Corporation, Albuquerque, New Mexico 87106, USA

C. Wagner

University of Michigan, Ann Arbor, Michigan 48109, USA

(Received 11 October 2018; published 5 December 2018)

Herein we present details of the design, simulation, and performance of a 100-GW linear transformer driver (LTD) cavity at Sandia National Laboratories. The cavity consists of 20 "bricks." Each brick is comprised of two 80 nF, 100 kV capacitors connected electrically in series with a custom, 200 kV, three-electrode, field-distortion gas switch. The brick capacitors are bipolar charged to ± 100 kV for a total switch voltage of 200 kV. Typical brick circuit parameters are 40 nF capacitance (two 80 nF capacitors in series) and 160 nH inductance. The switch electrodes are fabricated from a WCu alloy and are operated with breathable air. Over the course of 6,556 shots the cavity generated a peak electrical current and power of 1.03 MA ($\pm 1.8\%$) and 106 GW ($\pm 3.1\%$). Experimental results are consistent (to within uncertainties) with circuit simulations for normal operation, and expected failure modes including prefire and late-fire events. New features of this development that are reported here in detail include: (1) 100 ns, 1 MA, 100-GW output from a 2.2 m diameter LTD into a 0.1 Ω load, (2) high-impedance solid charging resistors that are optimized for this application, and (3) evaluation of maintenance-free trigger circuits using capacitive coupling and inductive isolation.

I. INTRODUCTION

The High Energy Density Physics (HEDP) community is proposing to build a next-generation pulsed-power accelerator with peak electrical output power in the range of 300 TW to 1,000 TW [1–6]. The prime power source of such a machine may consist of a system of linear transformer drivers (LTDs) [7–18] fast Marx generators (FMGs) [7,9,19–22] or impedance-matched Marx generators (IMGs) [18,23,24]. The pulsed power community has been developing LTD technology for 20 years on various single-cavity experiments [16,25–37], multicavity (single "module") experiments [14,27,32,35,38–44] and a few multimodule experiments [11,14]. The work presented here describes the design and performance of the first two meter diameter, 100-GW LTD cavity for application to future petawatt-class accelerators with additional focus on reliability and maintenance.

II. SYSTEM DESIGN

This design consists of a single 2.2 m diameter LTD cavity with 20 "bricks," top view is shown in Fig. 1. Each brick consists of two 80 nF capacitors that are charged to ± 100 kV (200 kV total) and separated by a 200-kV spark gap switch; a cross-sectional view of the component layout is shown in Fig. 2. The total series inductance of each brick is 160 nH. The 20 bricks are arranged in an annular configuration around the output electrodes of the cavity, as shown in Fig. 1. The cavity used in these experiments was repurposed from another device that was designed to operate with 24 bricks. Thus our experiments with 20 bricks have four brick positions inside the cavity that are

[*]jddougl@sandia.gov
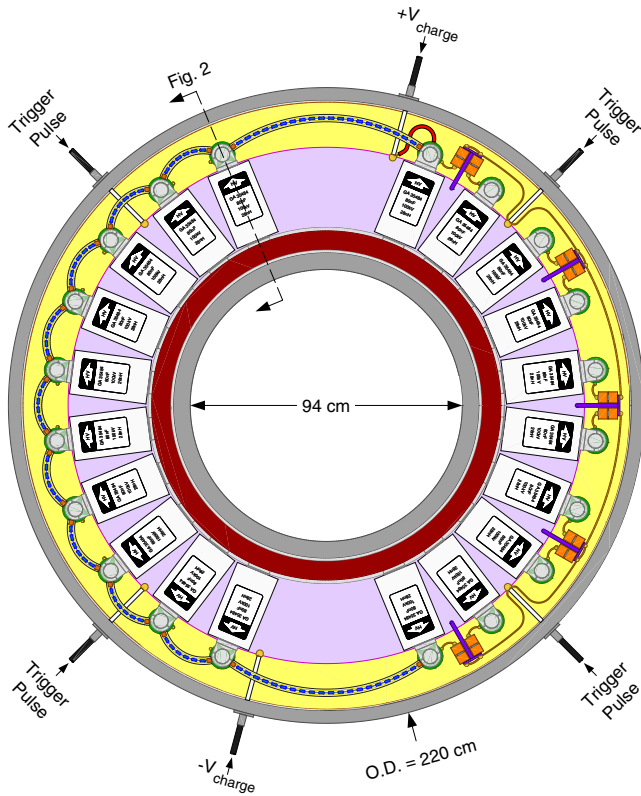
FIG. 1. Top-down illustration of the 100-GW "Z-Next" LTD with top lid and insulator removed. The right half of the illustration shows internal trigger circuitry with capacitive coupling (charging circuitry not shown), details are given in Fig. 5. The rest of the illustration shows details of the charging circuit (internal trigger circuitry not shown) that is described in Sec. II A. Fasteners and seals are omitted from this illustration. Component materials follow the legends shown in Figs. 2 and 5.

not populated. We chose to leave out the two bricks at the 12:00 and 6:00 positions (four total), as shown in Fig. 1. It is our convention to number the bricks starting from the 12:00 position and counting up in the counterclockwise direction. In order to maintain consistent brick numbering with future experiments using the same cavity with all 24 bricks populated we skip over positions 1, 12, 13 and 24 and thus number the first brick in our experiments as "2" and the last brick as "23". This numbering scheme will come into play in our discussion of experimental results.

A. Charging circuit

The physical layout of the charging system used with this LTD is similar to previous work [25,30,34]. A top-view illustration of the open cavity is shown in Fig. 1. The charging supply lines enter the cavity through two feed-throughs with one for each polarity (± 100 kV). Each supply coaxial cable connects to a receptacle on the middle insulator [Fig. 2(E)] for mechanical support. Insulated high-voltage jumper wires make connections from each of these receptacles to the nearest brick charging terminal of the respective polarity, as illustrated by the red wire in the top portion of Fig. 1. The internal charging circuitry consists of an annular ring of series-connected resistors for each supply polarity. The two rings of charging resistors are physically separated as much as possible toward the upper and lower cavity lids in order to prevent breakdown (200 kV at full charge). Aluminum clamps that primarily serve to connect the switch terminals to the capacitor output terminals (items Q and R in Fig. 2) also serve as nodes that connect the charging resistors together to form a continuous ring. The resistors, shown in Fig. 3, have a male banana
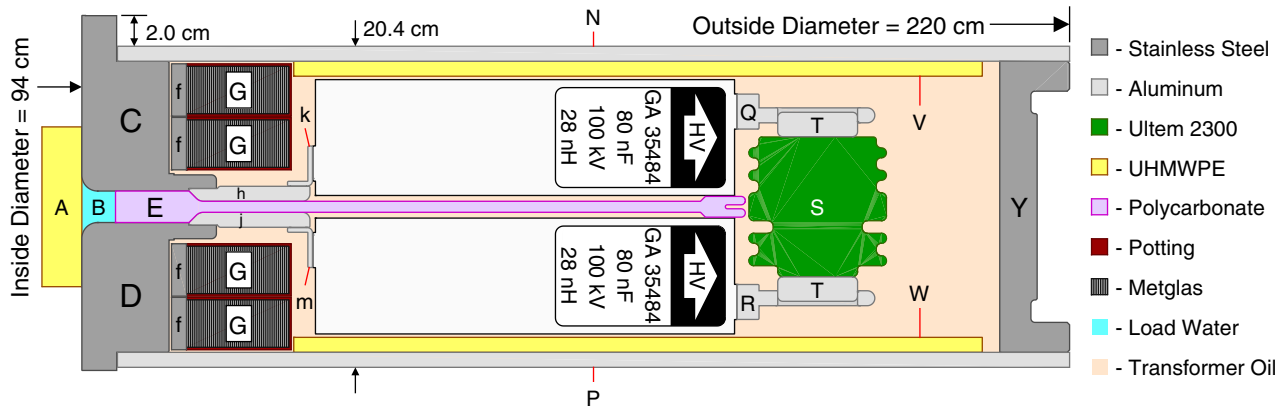
FIG. 2. Cross section (r-z plane) view of the 100-GW "Z-Next" LTD. (A) cylindrical load water insulating barrier, (B) cylindrical load water volume, (C) negative output electrode (cylindrical), (D) positive output electrode (cylindrical), (E) cylindrical "middle insulator", (f) cylindrical assembly mandrels for Metglas ribbon cores, (G) cylindrical, potted Metglas magnetic cores, (h) negative capacitor output bus (cylindrical), (j) positive capacitor output bus (cylindrical), (k) negative capacitor mounting bracket, (m) positive capacitor mounting bracket, (N) "top" LTD lid (cylindrical), (P) "bottom" LTD lid (cylindrical), (Q) positive charge terminal and switch mount, (R) negative charge terminal and switch mount, (S) 200 kV gas switch, (T) switch terminals, (V) "top" lid insulator (cylindrical), (W) "bottom" lid insulator (cylindrical), (Y) outer cylindrical wall of cavity. Component materials are as specified by the legend at right. The cylindrical axis of the assembly is to the left of the illustration. Charging circuitry, trigger circuitry, switch gas supply, load water supply, diagnostics, seals, and fasteners are omitted from this illustration.

FIG. 3. Photograph of a solid, high-impedance charging resistor. Each resistor (blue pills) is a 10 kΩ, 7.5 kV, axial package, P/N: RT818A103L from HVR. Resistor housing is Tygon tube. The tube is filled with highly-processed transformer oil, degassed over night and then sealed with copper end-plugs and plastic clamps. End connections vary; this assembly uses banana plugs where others use fork terminals, ring lugs, etc.

plug at each end; the aluminum switch clamps have female banana receptacles.

The charging resistors going to each brick are custom made from six 10 kΩ discrete high-voltage resistors connected in series. Each 60 kΩ resistor chain is encapsulated in a tygon tube that is degassed and filled with transformer oil to further inhibit breakdown. A sample photograph of this new resistor construction is shown in Fig. 3. The composition of these charging resistors has not been reported previously. This type of resistor, patented by Stoltzfus *et al.* [45], was invented to provide high-impedance with long-term stability and to avoid the problems that arise when using aqueous resistors, such as copper sulfate, in high-power LTDs [16,34,42,46]. Aqueous resistors are known to permeate water through their plastic housings contaminating the cavity and at the same time creating air bubbles inside the resistor that can dramatically change the impedance of the resistor and even create breakdowns inside the resistor. Previous work exists where monolithic solid resistors were used in place of conventional aqueous resistors but it was found that these would occasionally disintegrate or degrade [34,46]. Recent work has also been done by Zhou *et al.* [16] that uses wire-coil "spring" inductors instead of aqueous resistors for charging and triggering.

Our new resistor design, shown in Fig. 3, consisting of a chain of solid (axial package) resistors in oil-filled tygon tubing, is commonly used on brick-based pulsed power drivers at Sandia National Labs. On previous LTDs with 500 Ω to 1.5 kΩ charging resistors [25,30,34] it was found that when a single switch prefired that all of the capacitors in the cavity would discharge through the single offending switch, potentially causing switch damage and thereby increasing the probability of future prefires. By increasing the charging resistor values to at least 50 kΩ insufficient current is delivered to a prefiring switch from neighboring capacitors to maintain conduction, i.e., the arc extinguishes. High-impedance aqueous resistors, of the conventional design used in LTDs, are susceptible to degradation, i.e., changes in the solution resistivity. The new solid design provides a high-impedance (for switch decoupling during a prefire), high-voltage resistor that is stable, maintenance

free, fairly simple to construct, and does not contaminate the cavity by permeating water.

B. Trigger circuit

Descriptions of other LTD trigger configurations are given in Refs. [16,28,31,34,36,37,42,46–49], all of which, with the exception of Zhou *et al.*, use aqueous resistors in their trigger circuits for switch-to-switch isolation and circuit protection. An example of this circuit including typical component values is shown in Fig. 4. The use of aqueous resistors in the trigger circuit, as with the charging circuit described in Sec. II A, is problematic due to water permeation and bubble formation [16,34,42,46], which in the extreme leads to complete dehydration of the resistor assemblies. Degradation of aqueous trigger resistors (increasing impedance) will eventually prevent brick switches from firing on command which decreases driver output amplitude and increases pulse rise-time. Thus, LTDs that use aqueous trigger resistors periodically need to be refurbished with new resistors; for systems at Sandia this is generally an annual requirement. In order to eliminate these issues in the experiments reported here a new trigger circuit was evaluated that used ceramic "doorknob" capacitors in place of the conventional aqueous isolation resistors. Ultimately it was found that a trigger circuit with inductive isolating elements, as reported by Joseph [50] and Zhou [16], produced the best LTD performance.

The internal trigger circuit of this 20-brick LTD is divided into four identical quadrants; a single quadrant of the trigger circuit with capacitive DC isolation is illustrated in Fig. 5. Coaxial cables carry synchronous trigger pulses (from the same trigger generator) to each of the four quadrants through external penetrations of the LTD outer cylindrical wall at locations separated by 90° in azimuth, as shown in Fig. 1. Each of the four trigger pulses entering the cavity is fanned out to five bricks by a solid copper bus wire suspended in transformer oil that is routed in the space between the brick switches and outer cavity wall. A connection is made from this trigger bus wire to each switch trigger electrode by an isolating element, be it resistive, capacitive or inductive, that completes the trigger circuit routing. The trigger generator used in these experiments produced a 20 ns rising pulse with peak amplitude as high as 100 kV (positive polarity applied to switch trigger electrodes), the basic circuit elements are given in Fig. 4.

One of the primary goals of this development was to demonstrate a high-power LTD with minimal maintenance requirements that would be suitable for a many-cavity LTD module. As such, the maintenance-free capacitively isolated trigger circuit was used from the start of experimentation. In this configuration each switch is DC-isolated from the trigger bus through two series-connected, 560 pF, 50 kV "doorknob" ceramic capacitors (TDK UHV-10A), as shown in Fig. 5. A scan of the trigger generator charge
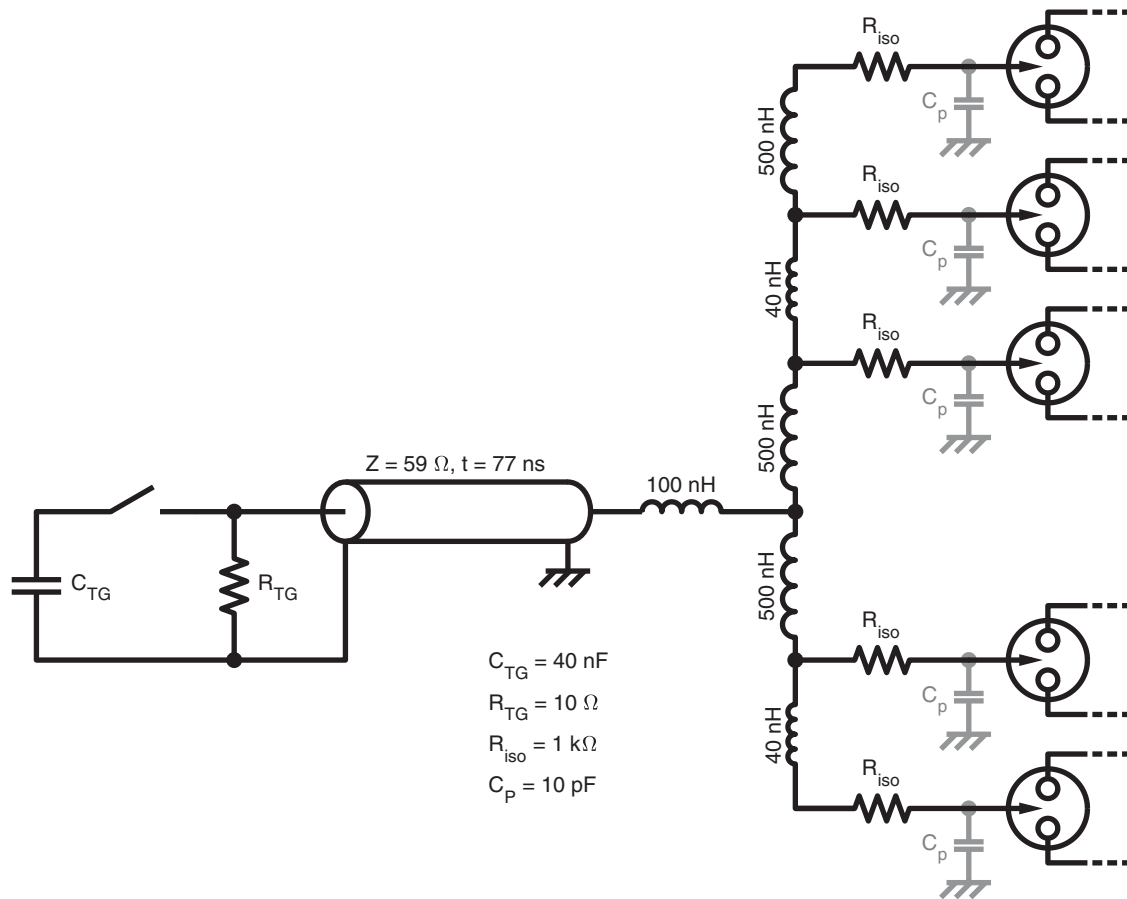
FIG. 4. Conventional LTD trigger circuit using aqueous resistors (R_{iso}) for isolating elements between switches and for circuit protection.

voltage found 84 kV to be the optimal trigger voltage setting in that the lowest switch late-fire rate was observed.

After over 4,750 full-voltage (± 100 kV) shots there have been zero failures of components in this novel trigger design. The capacitively-coupled trigger proved to be reliable and maintenance-free. However, with this trigger circuit configuration switch gas pressure had to be increased higher than expected to suppress prefires (presumably due to floating trigger electrodes) and the switch late-fire rate increased accordingly. The increased late-fire rate was strongly correlated with switch position on the trigger bus. The switches in each trigger quadrant with the most inductive isolation due to trigger bus wire parasitic inductance (the upper most switch in the schematic shown in Fig. 4) essentially never late-fired in over 4,500 shots, leading us to the conclusion that the lack of switch-to-switch trigger isolation inherent to the capacitively coupled circuit (without additional isolating inductance or resistance) is detrimental to LTD performance.

The capacitively coupled trigger circuit provides excellent DC isolation but very little transient isolation between neighboring switches whose trigger electrode connections "T" off of the trigger bus wire at nearly coincident points,

i.e., with very little parasitic inductive isolation provided by the trigger bus wire. The lack of transient isolation results in poor tolerance to switch jitter which manifests as increased probability of late-firing switches. To better understand the issue we briefly examine the process of switch closure in a three-electrode field-distortion gas switch: (1) Switch output electrodes are biased to some potential, $\pm V_{\mathrm{chg}}$ for example, the trigger electrode is biased to the mean output electrode voltage, zero volts in this case (2) Voltage is applied to the trigger electrode to overstress one of the gaps and induce breakdown, closing the overstressed gap (3) Closure of the overstressed gap forces the voltage on the trigger electrode to change drastically, nearly reaching the voltage of the output terminal associated with the closed gap (4) With the trigger electrode voltage now near the closed output terminal voltage the remaining gap is now overstressed and breaks down resulting in complete switch closure.

Switch jitter is the random variation in the amount of time it takes for the two gaps of the switch to breakdown once they are overstressed. In the case of an LTD multiple switches are triggered in parallel. Without sufficient isolation between switch trigger terminals the first gap closure
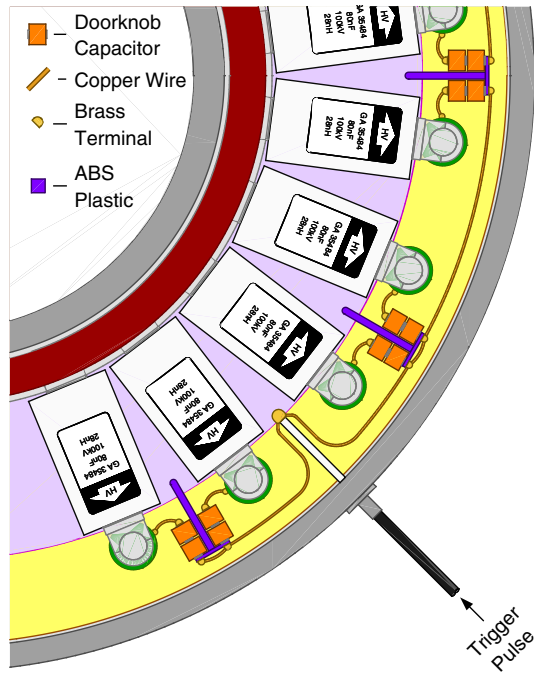
FIG. 5. Top-down view of the 100-GW "Z-Next" LTD trigger circuit layout with capacitive coupling (top lid and lid insulator removed). This configuration is mirrored up-down and right-left about the cavity to complete the trigger circuitry to all quadrants of the LTD. Component materials follow the legend given in Fig. 2. Charging circuitry, gas lines, load hardware, fasteners, and seals are omitted from this illustration.

of one switch can force the voltage on the trigger terminal of a neighboring switch (through the common trigger bus wire) to a voltage insufficient to trigger, possibly causing a late-fire. The conventional method to prevent this situation is by resistive isolation, typically $500\ \Omega$ to $1.5\ \text{k}\Omega$, as shown in Fig. 4. The added resistance in combination with typical switch parasitic capacitance of 10 pF produces an RC circuit with characteristic time scale of about 20 ns $(2R_{\text{iso}}C_p)$, easily providing tolerance to about 5 ns of switch jitter which is much more than what is typical for this type of switch.

The case of our capacitively coupled trigger circuit is much different. There is no significant resistance in the circuit and the series doorknob capacitors are effectively short circuits to nanosecond scale transients. The only form of switch-to-switch trigger isolation is from the parasitic inductance of the wiring and capacitance of the switch gaps. The zero-to-peak (quarter-cycle) time scale of this LC circuit for our geometry is less than 2 ns $(\frac{\pi}{2}\sqrt{LC})$, which is comparable to typical switch jitter.

The use of wire-wound inductors provides much greater isolation inductance than the purely parasitic (capacitively coupled) circuit. In our case we use inductors of about $8\ \mu\text{H}$, which yields an LC circuit with zero-to-peak time scale of about 20 ns $(\frac{\pi}{2}\sqrt{2L_{\text{iso}}C_p})$. The inductively isolated

circuit has isolation on par with the resistive circuit but has unique benefits. First, the inductive circuit exhibits higher ringing voltage gain at the switch trigger terminals, this effectively allows operation at lower trigger generator charge voltage and/or higher switch gas pressures to decrease prefire probability. Second, the wire-wound inductor is inexpensive and unlike the aqueous resistor it is maintenance-free.

Using the same switch gas pressure and trigger generator charge voltage as was typical for operation with the capacitively coupled trigger not a single prefire or late-fire occurred in nearly 150 shots using the inductively isolated LTD trigger circuit. Experiments are ongoing with reduced gas pressure (1.57 vs 1.70 MPa) and trigger generator charge voltage (60 kV vs 84 kV). Complete results are given in Fig. 6, results emphasizing the results from inductive isolation are shown in Fig. 10.

C. Magnetic cores

There are four magnetic cores inside this LTD. The cores are composed of Metglas 2605CO ribbon and the construction is very similar to that used in the LTD-III experiment at Sandia [34]. New cores were fabricated to fit the specific geometry of this cavity. The Metglas ribbon is 3 cm wide and $23\ \mu\text{m}$ thick. The core windings are insulated by $4\ \mu\text{m}$ mylar, the cross-sectional dimensions of each wound core is about 3×6.5 cm, potting then adds 1.6 mm on each side; the inside diameter is 107.3 cm.

D. Gas supply

Two external penetrations are made for the gas supply lines running to each switch (one for fill, one for purge). Hence, there are 40 external penetrations in the outer cylindrical wall of the LTD cavity for gas lines. External manifolds aggregate the numerous gas lines into single main fill and purge lines. Depending on the trigger circuit in use typical switch pressure is 1.57 MPa to 1.70 MPa (215 psig to 235 psig) using bottle supplied "Zero-air." In order to discourage prefires (according to the experience of machine operators) gas is thoroughly purged after every shot by opening fill and vent valves simultaneously until the gas flow, which is initially strong and turbulent, reaches a calm steady flow that is limited by the conductance of the gas lines. For our configuration the purge duration is typically ten seconds. Results from gas pressure scans are given in Fig. 6.

E. Diagnostics

System diagnostics include V-dot probes directed at the trigger electrode of each switch and B-dot probes at the output connections of each brick. V-dot connections are made by external penetrations of the outer cavity wall at each brick location. B-dots are installed in the output electrodes of the cavity centered at the azimuthal location
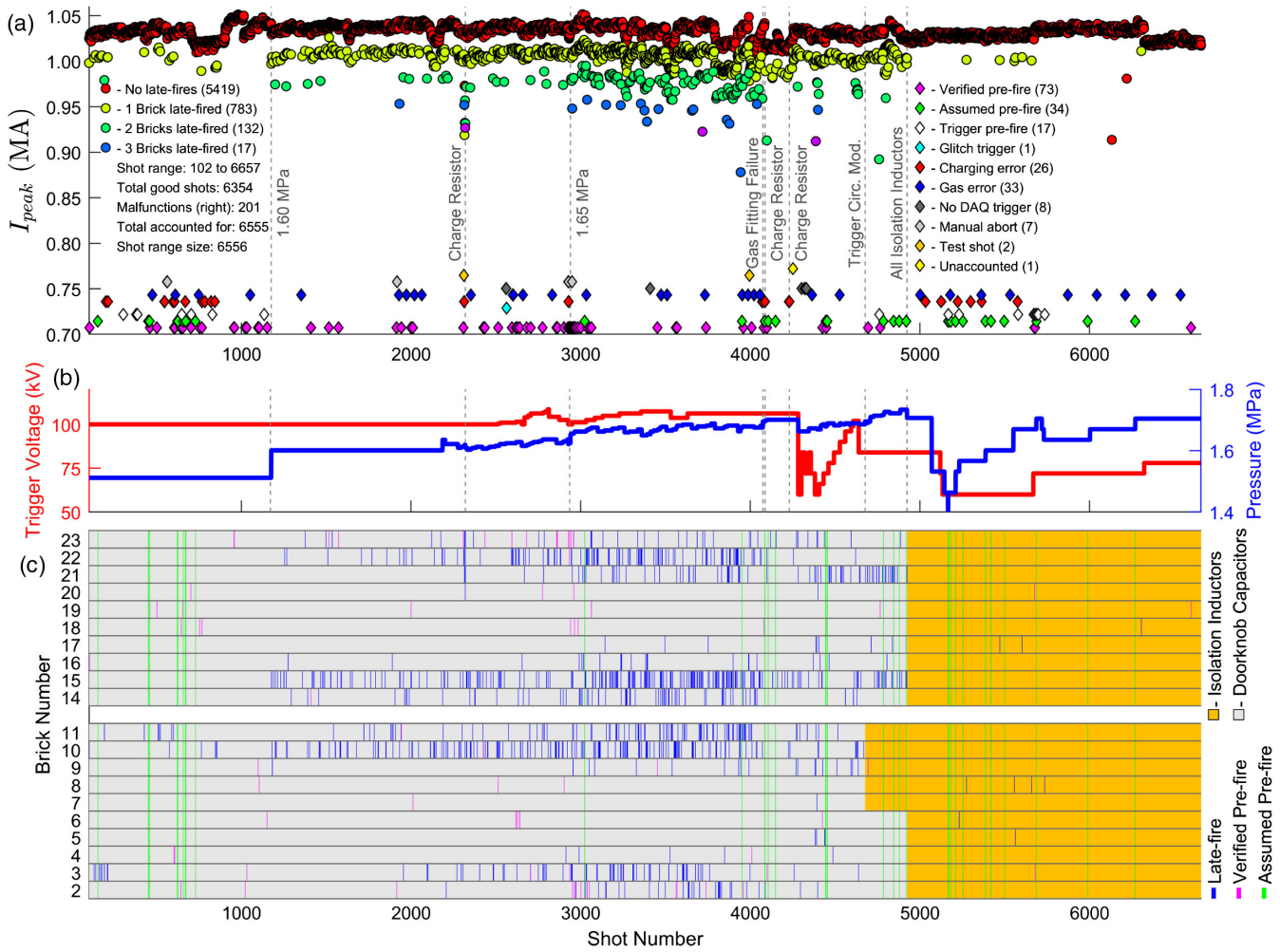
FIG. 6. 100-GW LTD complete history for ±100 kV operation. The top plot (a) indicates the peak current from the LTD for every shot where a malfunction did not occur; every occurrence of a malfunction is indicated along the horizontal axis, vertical spread is for clarity, peak current is generally near zero and irrelevant for malfunctions. The middle plot (b) shows the switch gas pressure and trigger generator charge voltage for each shot. The lower plot (c) indicates occurrences of prefires and late-fires as a function of brick position, shot number, and trigger circuit configuration.

of each brick. B-dot connections are made to external signal cables through penetrations in the cavity lid very near the inside radius (output electrode) of the cavity. The B-dot signal calibration is derived from total load current into a standard monitor. Both types of monitor are sampled by an oscilloscope-based data acquisition system with sample rate of 2 gigasamples/s on each channel.

Total load current is taken as the average of the numerically integrated B-dot signals from each brick.

III. CIRCUIT SIMULATIONS OF THE 100 GW LTD

Circuit simulations of this LTD were carried out using Micro-Cap with the equivalent LTD circuit shown in Fig. 7, as done in Refs. [25,27,29,31,32,41]. The values used for the lumped components of Fig. 7 are $C_{\mathrm{LTD}} = 20 \times 42$ nF (840 nF), $R_{\mathrm{LTD}} = 7$ mΩ, $L_{\mathrm{LTD}} = 8.2$ nH, $R_{\mathrm{core}} = 2.5$ Ω, $L_{\mathrm{load}} = 0.1$ nH, and $R_{\mathrm{load}} = 0.1$ Ω. These component

values are in good agreement with single-brick testing (C_{LTD}, R_{LTD}, and L_{LTD}), estimates from geometric calculation (L_{load}), experimental measurements (R_{load}), and previous work (R_{core}) [34]. Simulation output is in good agreement with experimental results, a sample of which is shown in Fig. 8.
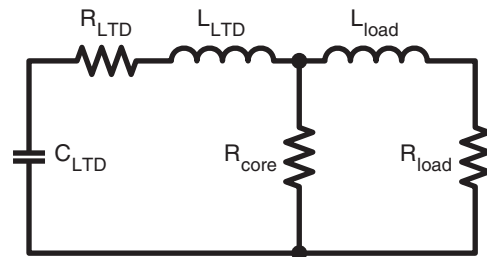
FIG. 7. Simplified equivalent circuit of the LTD with core losses.
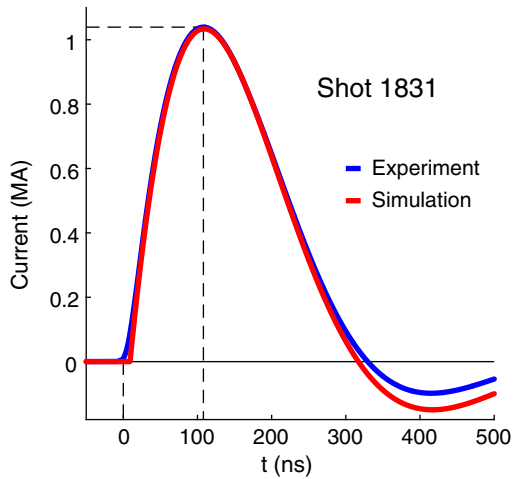
FIG. 8.   Comparison of output current from simulation and experiment. Simulation result is from the circuit show in Fig. 7 using the component values listed in Sec. III with an initial charge voltage of 200 kV.

IV. EXPERIMENTAL RESULTS

A. Output performance

Testing of the 100-GW LTD cavity was conducted off-and-on over a period of nine months and consisted of 6,556 shots, all of which were at ± 100 kV charge. The average peak output current from these tests, excluding aborted shots and malfunctions other than late-fires, was 1.03 MA $\pm$ 1.8% (1-σ). The average peak output power, also excluding aborted shots and malfunctions other than late-fires, was 106 GW $\pm$ 3.4% (1-σ). The experimentally measured output current and power from shot 2,555 are shown in Fig. 9. Performance results and operational parameters for the entire experimental campaign to date are shown in Fig. 6.
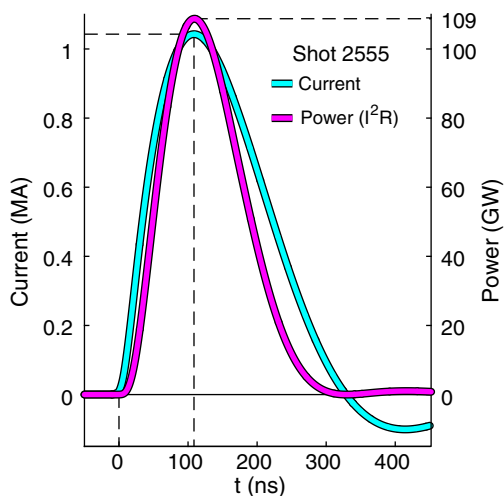
FIG. 9.   Sample plot of output current and power from the 100-GW LTD experiment.

B. System reliability

In addition to validating the output performance and variability another objective of this effort was to establish component reliability and longevity. During this run of 6,556 shots there were several significant component failures that required the cavity to be opened for repairs. These failures are as follows: (i) Brick capacitor—one failure after over 4,000 shots (ii) Broken gas fitting at switch housing—(shot 4,686) oil entered gas line and cross-contaminated five switches (one entire quadrant) (iii) Destroyed charge resistors—long-leg charge resistor failures at approximately 1,000 shot intervals. The cause of this failure has been identified and it is not related to the new resistor design. With the exception of two short-leg charge resistors oriented entirely vertically, no short-leg charge resistors of the new solid high-impedance design have failed over the 6,556 shot history of the 100-GW LTD.

C. Aborted shots and system malfunctions

These data were obtained with an intershot period of two to three minutes. The operation (charging, gas purge and fill, core reset), firing, and data acquisition (DAQ) for the cavity were performed by an automated control system. Various conditions for aborting shots in the course of normal operation and some system malfunctions have occurred on the 100-GW LTD experiment over 6,556 shots to date. All conditions for aborting a shot and most system malfunctions are not related to the cavity design, reliability or performance and as such are not included in aggregate statistics such as average peak output current, power and variability. Every occurrence of an aborted shot and each type of malfunction is noted along the bottom axis of the upper plot in Fig. 6. The total number of occurrences of abort conditions and each type of malfunction are given in parenthesis in the right legend of Fig. 6, and below. Each abort condition and type of system malfunction are described here in detail.

Verified prefires (73) shots where the LTD spontaneously fired before the command trigger and signals recorded by the data acquisition confirm nonsynchronous switch closure; the switch where the prefire originated can be identified. The prefire causes charge voltage imbalance or similar error and the shot is automatically aborted. Prefires are not included in aggregate analyses because it is not known whether or not a successful shot would have resulted had the charge sequence not been aborted. This is discussed further below.

Assumed prefires (34) shots where the automated control system aborted the shot while charging and the LTD emitted a sound consistent with a verified prefire but the data acquisition system did not trigger or was triggered by a glitch and recorded flat traces on all channels. Note that the origin of assumed prefires could be in the LTD cavity or in the trigger generator, we cannot distinguish between the two in these cases. Shots can be aborted while in the

charging state due to positive and negative charge voltage imbalance and/or indication of breakdown from change (drop) in charge voltage. Pre-fires are not included in aggregate analyses because it is not known whether or not a successful shot would have resulted had the charge sequence not been aborted. This is discussed further below.

Trigger prefires (17) shots where the LTD fired before the command trigger and signals recorded by the data acquisition indicate synchronous closure of all switches. These conditions indicate that a prefire occurred in the trigger generator. The trigger prefire causes charge voltage imbalance or similar error and the shot is automatically aborted. Trigger prefires are not included in aggregate analyses because the source of the malfunction is not relevant to cavity reliability.

Glitch trigger (1) shots where data was recorded, there is no indication of prefire or late-fire, there is no indication of any other malfunction in the logbook and all signals are nearly zero for the entire record other than a slight blip of order 10 ns and slightly above the noise floor at the trigger time. In these cases we assume that the data acquisition system, which operates in single-sequence mode, was inadvertently triggered prior to the downline shot. These cases are very rare (one occurrence) and are not included in aggregate analyses.

Charging errors (26) shots aborted by the automated control system while in charging state. Abort conditions include gas pressure out of range, charge voltage imbalance out of range, and breakdown indicated by change (drop) in charge voltage. If there is indication of a verified or assumed prefire then shots are counted as prefires, not charge errors.

Gas errors (33) shots aborted prior to charging because the target LTD switch gas pressure and/or trigger generator switch pressure could not be reached. The LTD switch gas and trigger generator switch gas are supplied by bottles; when the bottles run low or if the bottles are not opened the shot is aborted due to gas error. These shots have no bearing on LTD performance or reliability and are not included in aggregate analyses.

No DAQ trigger (8) shots where all indications point to a successful downline shot but no data was recorded by the data acquisition system. These cases are all preceded by a change to the trigger circuit or trigger generator charge voltage without any change in the trigger threshold of the data acquisition system; trigger threshold compensation is made subsequently. Since no data exists for these shots they cannot be included in any analyses.

Manual abort (7) shots where the "Abort" button in the control interface was pressed. This is almost always unintentional. Intentional manual aborts include cases where gas lines external to the LTD cavity ruptured during gas fill. Since no data exists for these shots they cannot be included in any analyses.

Test shots (2) shots made to verify repairs or modifications to systems external to the LTD cavity. For these cases the cavity is not charged. These include verification of replaced trigger generator capacitors and verification of new trigger threshold settings. These cases are not true shots and have no bearing on LTD performance or reliability and are not included in aggregate analyses.

Unaccounted (1) shots where no data was recorded and there are no comments in the logbook. Since no data exists for these shots they cannot be included in any analyses.

D. Switch prefire rate

Quantifying the prefire rate of this experiment is not entirely straightforward. The automated data acquisition system operates in single-sequence mode and is triggered by a signal from a voltage monitor connected to the output of the trigger generator. Prefires that occur near full charge voltage induce sufficient signal in the trigger generator output voltage monitor to trigger the data acquisition system; in this case it can be verified that a prefire did occur (as opposed to some other type of malfunction) and the prefiring switch can be identified, we refer to this as a "verified prefire." However, the inadvertent trigger signal produced by a prefire does not always trigger the data acquisition, particularly if it occurs earlier during the charge sequence. When this happens the result is usually an imbalance in the positive and negative charge voltages which causes the shot to be aborted by the automated control system. In this case we have no way to determine where the malfunction originated and the sound emitted by the LTD, i.e., popping, is the only indication of the type of malfunction (prefire or other) that occurred, we refer to this case as an "assumed prefire." Note that assumed prefires may have occurred in the cavity or in the trigger generator; without captured data we cannot distinguish between the two. It is also possible for a prefire to be so insignificant that the shot does not abort, charging continues and a successful shot is eventually recorded as the result of the experiment; this case is the most uncommon of the three, highly speculative and is the least serious, as such we do not count these cases as prefires.

These various scenarios complicate our assessment of the LTD prefire rate. The resulting ambiguity is conveyed by the lower plot in Fig. 6 where vertical green and magenta lines indicate prefire events; vertical green lines extending across all brick numbers are assumed prefires that did not trigger the data acquisition and hence the offending switch could not be identified; short magenta lines limited to a specific brick number are verified prefires that triggered the data acquisition system. To date, there have been 73 verified prefires and 33 assumed prefires in 6,556 shots (131,120 switch shots). The physical distribution within the cavity of verified prefires is shown in Fig. 11, all but two of which occurred while using the capacitively coupled trigger circuit.

Using switch gas pressure and trigger voltage settings of 1.67 MPa (230 psig) and 84 kV with the inductively isolated trigger circuit the LTD has never experienced a prefire of any kind along with zero late-firing switches, see Sec. IV E. These
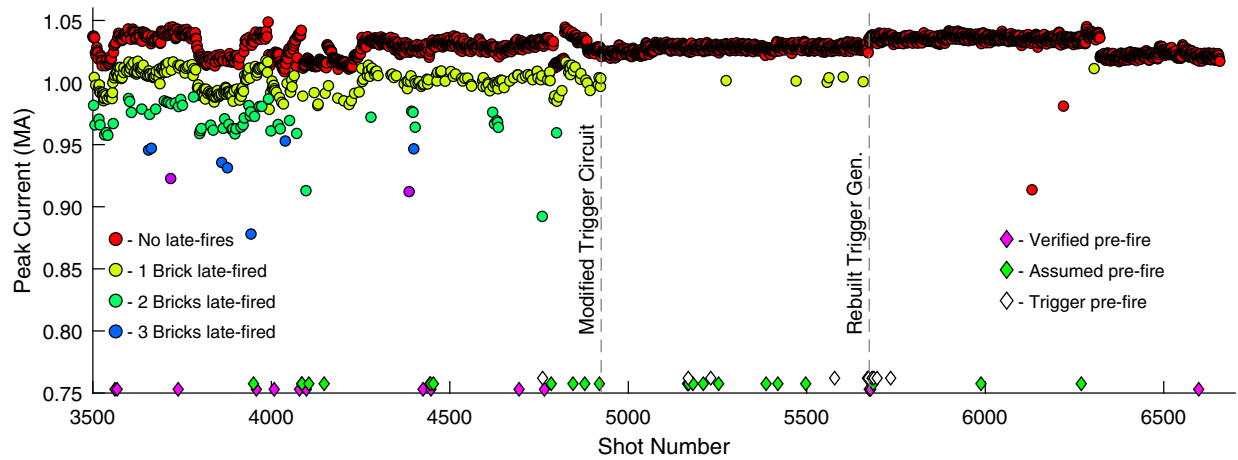
FIG. 10. Peak current and prefire events from the 100-GW LTD cavity from shots 3,500 to 6,657. Step discontinuities in the peak current are a result of day-to-day variations in load water resistivity.

settings span shots 4924 through 5069, 146 consecutive shots. Results from the most recent shots on the 100-GW cavity use reduced gas pressure and trigger voltage. For the 1,734 shots since converting to inductive trigger isolation there have been two verified prefires, one of which is likely due to a compromised trigger generator which allowed the switch trigger electrodes to float while charging. The most recent experimental results are shown in Fig. 10.

In addition to demonstrating an operating regime that is free of prefires and late-fires (Sec. IV E) we have developed other technology to mitigate the impact of prefires. Use of the high impedance charging resistors described in Sec. II A dramatically decreases the impact of a prefire by decreasing the amount of energy unintentionally delivered to the load and limiting switch current and charge transfer to typical shot levels thus preventing component damage. Hence, even in the extremely unlikely case that a prefire does occur it can be viewed as a "soft" failure. Should a cavity in a many-cavity module suffer from incurable prefiring (or other

chronic malfunction) it could be taken offline by disconnecting its charge lines and flooding the cavity with conductive liquid (in place of transformer oil), thus allowing the module to operate albeit with decreased performance.

E. Switch late-fire rate

Prior to the use of isolation inductors in the LTD trigger circuit the primary source of output pulse variation was late-firing switches, as demonstrated in the upper plot of Fig. 6. As discussed in Sec. II B and shown in Fig. 10, reconfiguring the trigger circuit with isolation inductors instead of capacitive coupling reduced the switch late-fire rate from 1.2% to 0.02% (LTD late-fire rate is 0.4%), the peak output current is now 1.03 MA $\pm$ 1.2% (1-σ). These aggregate quantities include 1,733 shots, most of which were taken during gas pressure and trigger voltage optimization campaigns where the late-fire rate is certainly higher than normal. The physical distribution within the cavity of late-fires for the different trigger circuits is shown with better clarity in Fig. 12. The output pulse shape of the LTD is now so consistent that the effect of small fluctuations in the ambient laboratory temperature (from HVAC) are clearly observable in the output pulse magnitude. Day-to-day drift in load water resistivity is now the primary contributor to output variation; this appears as step discontinuities in the peak output current in Fig. 10. Since adjustments of load water resistivity are only made at the beginning of each day of experiments the intraday variability in performance is more meaningful than the variability over multiple days of experiments. The average intraday variability in peak output current prior to implementation of the trigger isolation inductors was $\pm1.3\%$ (59 days of operation), with the inductive trigger isolation it is now $\pm0.32\%$ (1-σ, 18 days of operation). The only negative result of the isolation inductors has been turn-to-turn shorting in coils where adjacent turns were unintentionally in direct contact with each other.
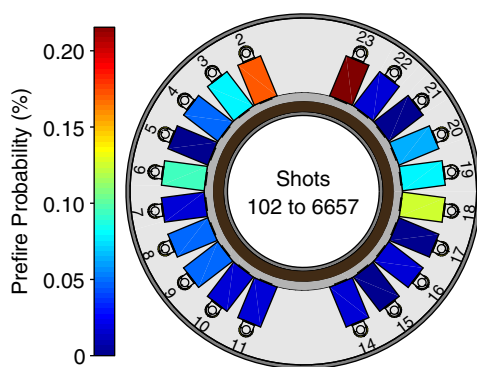
FIG. 11. Distribution of identifiable prefire events in the 100-GW LTD cavity. The plot shows probability (in percent) of a "verified" prefire at each of the 20 bricks in the cavity over the course of about 6,556 shots. For the most recent 1,733 shots there has only been two verified prefires, as shown in Fig. 10.
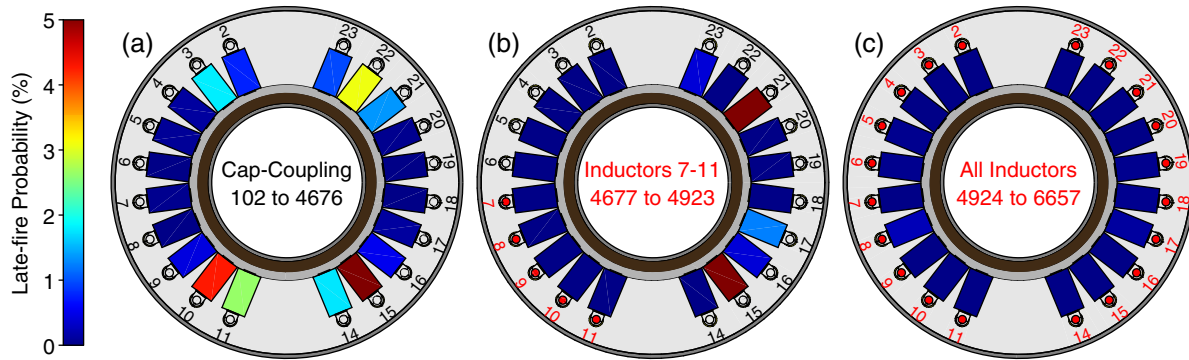
FIG. 12. Distribution of late-fire events in the 100-GW LTD cavity. Each plot shows the probability (in percent) of a late-fire at each of the 20 bricks in the cavity over a particular range of shots and trigger circuit configuration. The left plot (a) is late-fires from shots where all bricks used capacitive trigger coupling. The center plot (b) is a range of shots where bricks seven through 11 used inductive trigger isolation, all others remained capacitively coupled. The right plot (c) is late-fires from shot 4924 to present where all bricks use the inductively isolated trigger circuit.

While we have accomplished an excellent late-fire rate with this LTD it should be noted that a late-fire rate at or very near zero is not a requirement for a many-cavity LTD module. Having one late switch in the 20-brick LTD typically decreases peak output current by about 3%. For a multicavity module with a late-fire probability of 5% per cavity (more than an order of magnitude worse than we have obtained) we would expect typical decrease in output performance of less than 1% due to late-firing switches.

V. SUMMARY AND FUTURE WORK

The purpose of this research was to demonstrate that the performance and reliability required from a single-cavity LTD that would serve as the fundamental building block for a petawatt-class accelerator is attainable. We have succeeded in demonstrating the output performance for such a device with the "Z-Next" 100-GW LTD. By eliminating aqueous resistors from the charging and triggering systems we have eliminated all regular maintenance requirements of the LTD while improving output consistency of an LTD operating at ±100 kV charge to an unprecedented level of $\pm0.3\%$. These results bode very well for an N-cavity LTD module where random output variation is expected to be further reduced by a factor of $1/\sqrt{N}$.

The next major step in the Z-Next development campaign is to construct a two-to-five cavity module to demonstrate the performance and reliability of such a device and to resolve any unforeseen issues that should accompany the transition to a multicavity driver of this size and power density.

ACKNOWLEDGMENTS

[1] D. Cook, Z, ZX, and X-1: a realistic path to high fusion yield, in *Digest of Technical Papers, 12th IEEE International Pulsed Power Conference (Cat. No. 99CH36358)* (1999), Vol. 1, pp. 33–37, DOI: 10.1109/PPC.1999.825419.

[2] K. W. Struve, J. P. Corley, D. L. Johnson, D. H. McDaniel, R. B. Spielman, and W. A. Stygar, ZX pulsed-power design, in *Digest of Technical Papers, 12th IEEE International Pulsed Power Conference (Cat. No. 99CH36358)* (1999), Vol. 1, pp. 493–496, DOI: 10.1109/PPC.1999.825518.

[3] W. A. Stygar *et al.*, Theoretical z-pinch scaling relations for thermonuclear-fusion experiments, Phys. Rev. E **72**, 026404 (2005).

[4] C. L. Olson *et al.*, Recyclable transmission line (RTL) and linear transformer driver (LTD) development for Z-pinch inertial fusion energy (Z-IFE) and high yield, Sandia National Laboratories Technical Report No. SAND2007-0059, 2007.

[5] M. E. Cuneo *et al.*, Magnetically driven implosions for inertial confinement fusion at sandia national laboratories, IEEE Trans. Plasma Sci. **40**, 3222 (2012).

[6] S. A. Slutz, W. A. Stygar, M. R. Gomez, K. J. Peterson, A. B. Sefkow, D. B. Sinars, R. A. Vesey, E. M. Campbell, and R. Betti, Scaling magnetized liner inertial fusion on Z and future pulsed-power accelerators, Phys. Plasmas **23**, 022702 (2016).

[7] P. Corcoran, I. Smith, P. Spence, A. R. Miller, E. Waisman, C. Gilbert, W. Rix, P. Sincerny, L. Schlitt, and D. Bell, Pulse power for future X-ray simulators, in *PPPS-2001 Pulsed Power Plasma Science 2001, 28th IEEE International Conference on Plasma Science and 13th IEEE International Pulsed Power Conference, Digest of Papers (Cat. No. 01CH37251)* (2001), Vol. 1, pp. 577–581, DOI: 10.1109/PPPS.2001.1002161.

[8] M. G. Mazarakis, R. B. Spielman, K. W. Struve, and F. W. Long, Ultrafast LTD's for bremsstrahlung diodes and Z-pinches, in *PPPS-2001 Pulsed Power Plasma Science 2001, 28th IEEE International Conference on Plasma Science and 13th IEEE International Pulsed Power Conference, Digest of Papers (Cat. No. 01CH37251)* (2001), Vol. 1, pp. 587–590, DOI: 10.1109/PPPS.2001 .1002163.

[9] I. Smith, P. Corcoran, A. R. Miller, V. Carboni, P. Sincerny, P. Spence, C. Gilbert, W. Rix, E. Waisman, L. Schlitt, and D. Bell, Pulse power for future and past X-ray simulators, IEEE Trans. Plasma Sci. **30,** 1746 (2002).

[10] A. Bastrikov, V. Vizir, S. Volkov, V. Durakov, A. Efremov, V. Zorin, A. Kim, B. Kovalchuk, E. Kumpjak, S. Loginov *et al.*, Primary energy storages based on linear transformer stages, Laser Part. Beams **21,** 295299 (2003).

[11] F. Lassalle, A. Loyen, A. Georges, B. Roques, H. Calamy, C. Mangeant, J. F. Cambonie, S. Laspalles, D. Cadars, G. Rodriguez, J. M. Delchie, P. Combes, T. Chanconi, and J. Saves, Status on the SPHINX machine based on the 1 microsecond LTD technology, in *2007 16th IEEE International Pulsed Power Conference* (2007), Vol. 1, pp. 217–221, DOI: 10.1109/PPPS.2007.4651825.

[12] W. A. Stygar, M. E. Cuneo, D. I. Headley, H. C. Ives, R. J. Leeper, M. G. Mazarakis, C. L. Olson, J. L. Porter, T. C. Wagoner, and J. R. Woodworth, Architecture of petawatt-class *z*-pinch accelerators, Phys. Rev. ST Accel. Beams **10,** 030401 (2007).

[13] W. A. Stygar, W. E. Fowler, K. R. LeChien, F. W. Long, M. G. Mazarakis, G. R. McKee, J. L. McKenney, J. L. Porter, M. E. Savage, B. S. Stoltzfus, D. M. Van De Valde, and J. R. Woodworth, Shaping the output pulse of a linear-transformer-driver module, Phys. Rev. ST Accel. Beams **12,** 030402 (2009).

[14] B. M. Kovalchuk, A. V. Kharlov, E. V. Kumpyak, and A. A. Zherlitsyn, Pulse generators based on air-insulated linear-transformer-driver stages, Phys. Rev. ST Accel. Beams **16,** 050401 (2013).

[15] W. A. Stygar *et al.*, Conceptual designs of two petawatt-class pulsed-power accelerators for high-energy-density-physics experiments, Phys. Rev. ST Accel. Beams **18,** 110401 (2015).

[16] L. Zhou, Z. Li, Z. Wang, C. Liang, M. Li, J. Qi, and Y. Chu, Design of a 5-MA 100-ns linear-transformer-driver accelerator for wire array Z-pinch experiments, Phys. Rev. Accel. Beams **19,** 030401 (2016).

[17] R. Spielman, D. Froula, G. Brent, E. Campbell, D. Reisman, M. Savage, M. Shoup, W. Stygar, and M. Wisher, Conceptual design of a 15-TW pulsed-power accelerator for high-energy-density-physics experiments, Matt. Rad. Ext. **2,** 204 (2017).

[18] W. A. Stygar, K. R. LeChien, M. G. Mazarakis, M. E. Savage, B. S. Stoltzfus, K. N. Austin, E. W. Breden, M. E. Cuneo, B. T. Hutsel, S. A. Lewis, G. R. McKee, J. K. Moore, T. D. Mulville, D. J. Muron, D. B. Reisman, M. E. Sceiford, and M. L. Wisher, Impedance-matched Marx generators, Phys. Rev. Accel. Beams **20,** 040402 (2017).

[19] P. Sincerny, M. Danforth, C. Gilbert, A. R. Miller, T. Naff, W. Rix, C. Stallings, E. Waisman, and L. Schlitt, Concepts for an affordable high current imploding plasma generator, in *Digest of Technical Papers, 12th IEEE International Pulsed Power Conference (Cat. No. 99CH36358)* (1999), Vol. 1, pp. 479–483, DOI: 10.1109/PPC.1999.825515.

[20] I. Smith, V. Carboni, A. R. Miller, R. Crumley, P. Corcoran, P. W. Spence, W. H. Rix, W. Powell, P. S. Sincerny, J. Ennis, and D. Bell, Fast Marx Generator development for PRS drivers, in *PPPS-2001 Pulsed Power Plasma Science 2001, 28th IEEE International Conference on Plasma Science and 13th IEEE International Pulsed Power Conference, Digest of Papers (Cat. No. 01CH37251)*, Vol. 1 (2001) pp. 582–586, DOI: 10.1109/PPPS.2001.1002162.

[21] P. Sincerny, V. Carboni, K. Childers, P. Corcoran, J. Hammon, S. K. Lam, R. Miller, T. Naff, I. Smith, T. Tucker, J. Ennis, R. Cooper, D. Bell, and R. Davis, Fast discharge energy storage development for improving X-ray simulators, in *2002 14th International Conference on High-Power Particle Beams (BEAMS)* (2002), Vol. 1, pp. 77–80, DOI: 10.1063/1.1530806.

[22] S. K. Lam, A. R. Miller, L. L. Sanders, P. Sincerny, and T. Tucker, Fast discharge energy storage development for advanced X-ray simulators, IEEE Trans. Plasma Sci. **33,** 982 (2005).

[23] W. A. Stygar *et al.*, Conceptual design of a 10^{13}-W pulsed-power accelerator for megajoule-class dynamic-material-physics experiments, Phys. Rev. Accel. Beams **19,** 070401 (2016).

[24] W. Stygar *et al.*, Conceptual design of a 960-TW accelerator powered by impedance-matched Marx generators, in *2017 IEEE 21st International Conference on Pulsed Power (PPC)* (2017), pp. 1–8, DOI: 10.1109/PPC.2017.8291256.

[25] A. A. Kim, B. M. Kovalchuk, A. N. Bastrikov, V. G. Durakov, S. N. Volkov, and V. A. Sinebryukhov, 100 ns current rise time LTD stage, in *PPPS-2001 Pulsed Power Plasma Science 2001, 28th IEEE International Conference on Plasma Science and 13th IEEE International Pulsed Power Conference, Digest of Papers (Cat. No. 01CH37251)* (2001), Vol. 2, pp. 1491–1494, DOI: 10.1109/ PPPS.2001.1001840.

[26] A. A. Kim, A. N. Bastrikov, S. N. Volkov, V. G. Durakov, B. M. Kovalchuk, and V. A. Sinebryukhov, Development of the ultra-fast LTD stage, in *2002 14th International Conference on High-Power Particle Beams (BEAMS)* (2002), Vol. 1, pp. 81–84, DOI: 10.1063/1.1530807.

[27] A. A. Kim, M. G. Mazarakis, V. A. Sinebryukhov, B. M. Kovalchuk, V. A. Visir, S. N. Volkov, F. Bayol, A. N. Bastrikov, V. G. Durakov, S. V. Frolov, V. M. Alexeenko, D. H. McDaniel, W. E. Fowler, K. LeChien, C. Olson, W. A. Stygar, K. W. Struve, J. Porter, and R. M. Gilgenbach, Development and tests of fast 1-MA linear transformer driver stages, Phys. Rev. ST Accel. Beams **12,** 050402 (2009).

[28] B. M. Kovalchuk, A. V. Kharlov, V. B. Zorin, and A. A. Zherlitsyn, A compact submicrosecond, high current generator, Rev. Sci. Instrum. **80**, 083504 (2009).

[29] M. G. Mazarakis, W. E. Fowler, A. A. Kim, V. A. Sinebryukhov, S. T. Rogowski, R. A. Sharpe, D. H. McDaniel, C. L. Olson, J. L. Porter, K. W. Struve, W. A. Stygar, and J. R. Woodworth, High current, 0.5-MA, fast, 100-ns, linear transformer driver experiments, Phys. Rev. ST Accel. Beams **12**, 050401 (2009).

[30] X. Liu, F. Sun, T. Liang, X. Jiang, Q. Zhang, and A. Qiu, Experimental study on multigap multichannel gas spark closing switch for LTD, IEEE Trans. Plasma Sci. **37**, 1318 (2009).

[31] X. Liu, X. Jiang, F. Sun, T. Liang, Q. Zhang, and A. Qiu, Experimental study on synchronous discharge of ten multigap multichannel gas switches, IEEE Trans. Plasma Sci. **37**, 1943 (2009).

[32] M. G. Mazarakis, K. Ward *et al.*, High-current linear transformer driver development at sandia national laboratories, IEEE Trans. Plasma Sci. **38**, 704 (2010).

[33] J. R. Woodworth, W. E. Fowler, W. A. Stygar, M. E. Sceiford, M. G. Mazarakis, H. D. Anderson, M. J. Harden, J. R. Blickem, K. Ward, R. White, and A. A. Kim, Experiments with the 0.6-MA LTD-III accelerator cavity, in *2010 IEEE International Power Modulator and High Voltage Conference* (2010), pp. 163–165, DOI: 10.1109/IPMHVC.2010.5958319.

[34] J. R. Woodworth, W. E. Fowler, B. S. Stoltzfus, W. A. Stygar, M. E. Sceiford, M. G. Mazarakis, H. D. Anderson, M. J. Harden, J. R. Blickem, R. White, and A. A. Kim, Compact 810 kA linear transformer driver cavity, Phys. Rev. ST Accel. Beams **14**, 040401 (2011).

[35] M. G. Mazarakis *et al.*, Experimental validation of the first 1-MA water-insulated MYKONOS LTD voltage adder, in *2011 IEEE Pulsed Power Conference* (2011), pp. 625–628, DOI: 10.1109/PPC.2011.6191552.

[36] J. J. Leckbee, G. E. Pea, M. L. Kiefer, J. A. Alexander, B. S. Stoltzfus, J. L. Brown, H. Wigelsworth, F. E. White, and B. Bui, Comparison of trigger requirements for gas switches for linear transformer drivers, in *2014 IEEE International Power Modulator and High Voltage Conference (IPMHVC)* (2014), pp. 93–96, DOI: 10.1109/IPMHVC.2014.7287215.

[37] S. Fengju, Z. Jiangtao, L. Tianxue, W. Hao, J. Xiaofeng, W. Zhiguo, Y. Jiahui, and Q. Ai'ci, Trigger method based on internal bricks within cavities for Linear Transformer Drivers, in *2015 IEEE Pulsed Power Conference (PPC)* (2015), pp. 1–4, DOI: 10.1109/PPC.2015.7296925.

[38] A. A. Zherlitsyn, B. M. Kovalchuk, G. V. Smorudov, N. V. Tsoy, V. A. Vizir, and V. B. Zorin, Air insulated LTD for E-beam diode, in *Proceedings of the 15th International Symposium on High Current Electronics*, edited by B. Kovalchuk and G. Remnev (Institute of High Current Electronics, Tomsk, Russia, 2008), pp. 296–298, http://www.hcei.tsc.ru/conf/2010/cat/proc_2008/shce/296-298.pdf.

[39] A. V. Kharlov, B. M. Kovalchuk, E. V. Kumpyak, A. A. Zherlisyn, V. B. Zorin, G. V. Smorudov, F. Bayol, and F. Lassalle, in *Proceedings of the 16th Symposium on High Current Electronics*, edited by B. Kovalchuk and G. Remnev (Institute of High Current Electronics, Tomsk,

Russia, 2010), pp. 261–264, http://www.hcei.tsc.ru/conf/2010/cat/proc_2010/shce/261-264.pdf.

[40] J. Leckbee, S. Cordova, B. Oliver, T. Webb, M. Toury, M. Caron, R. Rosol, B. Bui, T. Romero, and D. Ziska, Linear Transformer Driver (LTD) research for radiographic applications, in *2011 IEEE Pulsed Power Conference* (2011), pp. 614–618, DOI: 10.1109/PPC.2011.6191550.

[41] E. A. Madrid, C. L. Miller, D. V. Rose, D. R. Welch, R. E. Clark, C. B. Mostrom, W. A. Stygar, M. E. Savage, D. D. Hinshelwood, and K. R. LeChien, Transmission line and electromagnetic models of the Mykonos-2 accelerator, in *2011 IEEE Pulsed Power Conference* (2011), pp. 902–905, DOI: 10.1109/PPC.2011.6191536.

[42] M. E. Savage, M. G. Mazarakis, K. R. LeChien, B. S. Stoltzfus, W. A. Stygar, W. E. Fowler, E. A. Madrid, C. L. Miller, and D. V. Rose, Temporally shaped current pulses on a two-cavity linear transformer driver system, in *2011 IEEE Pulsed Power Conference* (2011), pp. 844–849, DOI: 10.1109/PPC.2011.6191525.

[43] B. T. Hutsel, B. S. Stoltzfus, E. W. Breden, W. E. Fowler, P. A. Jones, D. W. Justus, F. W. Long, D. J. Lucero, K. A. MacRunnels, M. G. Mazarakis, J. L. Mckenney, J. K. Moore, T. D. Mulville, J. L. Porter, M. E. Savage, and W. A. Stygar, Millimeter-gap magnetically insulated transmission line power flow experiments, in *2015 IEEE Pulsed Power Conference (PPC)* (2015), pp. 1–5, DOI: 10.1109/PPC.2015.7296902.

[44] F. Guo, W. Zou, L. Liu, L. Chen, B. Wei, D. Liu, M. Wang, and W. Xie, Current transmission efficiency for conical magnetically insulated transmission line on a 1.0-MV linear transformer driver system, IEEE Trans. Plasma Sci. **43**, 2663 (2015).

[45] B. S. Stoltzfus, M. E. Savage, B. T. Hutsel, W. E. Fowler, K. A. MacRunnels, D. Justus, and W. A. Stygar, Solid-state resistor for pulsed power machines, US Patent No. US9514864B2 (2016).

[46] A. A. Kim, M. G. Mazarakis, V. A. Sinebryukhov, S. N. Volkov, V. M. Alexeenko, S. S. Kondratiev, and S. V. Vasiliev, Lifetime of the HCEI spark gap switch for linear transformer drivers, in *2015 IEEE Pulsed Power Conference (PPC)* (2015), pp. 1–4, DOI: 10.1109/PPC.2015.7296875.

[47] A. A. Zherlitsyn, B. M. Kovalchuk, and G. V. Smorudov, Capacitor units with air insulation for linear transformers, Instrum. Exp. Tech. **52**, 802 (2009).

[48] Z. Tu, K. Liu, J. Qiu, and Y. Lei, A new triggering technology based on inductive transformer for linear transformer driver (LTD) switches, IEEE Trans. Dielectr. Electr. Insul. **20**, 1279 (2013).

[49] Y. Zhao, L. Chen, and L. Zhou, A 216 cables synchronization trigger for linear transformer driver, in *2014 IEEE International Power Modulator and High Voltage Conference (IPMHVC)* (2014), pp. 63–66, DOI: 10.1109/IPMHVC.2014.7287208.

[50] N. R. Joseph, M. E. Savage, J. C. Stephens, J. A. Lott, B. A. Lewis, R. D. Thomas, M. A. Torres, and E. G. Holman, Enhancements to the short pulse high intensity nanosecond X-radiator (SPHINX) pulsed power system, in *2015 IEEE Pulsed Power Conference (PPC)* (2015), pp. 1–5, DOI: 10.1109/PPC.2015.7296969.